EARTH SURFACE PROCESSES AND LANDFORMS
Earth Surf. Process. Landforms **36,** 449–459 (2011)

Published online 21 July 2010 in Wiley Online Library
(wileyonlinelibrary.com) DOI: 10.1002/esp.2058

Geomorphic and cosmogenic nuclide constraints on escarpment evolution in an intraplate setting, Darling Escarpment, Western Australia

Sara Jakica,[1]* Mark C. Quigley,[2] Mike Sandiford,[1] Dan Clark,[3] L. Keith Fifield[4] and Abaz Alimanovic[1]
[1] School of Earth Sciences, The University of Melbourne, Melbourne, VIC, 3010 Australia
[2] Department of Geological Sciences, University of Canterbury, Christchurch 8041, New Zealand
[3] Geospatial and Earth Monitoring Division, Geoscience Australia, Canberra, ACT 2609, Australia
[4] Research School of Physics and Engineering, Australian National University, Canberra, ACT 2601, Australia

Received 21 August 2008; Revised 4 March 2010; Accepted 11 April 2010

*Correspondence to: Sara Jakica, School of Earth Sciences, The University of Melbourne, Melbourne, VIC, 3010, Australia. E-mail: s.jakica@pgrad.unimelb.edu.au

ESPL
Earth Surface Processes and Landforms

ABSTRACT: The ~900 km long Darling Scarp in Western Australia is one of the most prominent linear topographic features on Earth. Despite the presence of over-steepened reaches in all westerly flowing streams crossing the scarp, and significant seismic activity within 100 km of the scarp, there is no historical seismicity and no reported evidence for Quaternary tectonic displacements on the underlying Darling Fault. Consequently, it is unclear whether the scarp is a rapidly evolving landform responding to recent tectonic and/or climatic forcing or a more slowly evolving landform. In order to quantify late Quaternary rates of erosion and scarp relief processes, we obtained measurements of the cosmic-ray produced nuclide beryllium-10 (^{10}Be) from outcropping bedrock surfaces along the scarp summit and face, in valley floors, and at stream knickpoints. Erosion rates of bedrock outcrops along the scarp summit surface range from 0·5 to 4·0 m Myr^{-1}. These are in the same range as erosion rates of 2·1 to 3·6 m Myr^{-1} on the scarp face and similar to river incision rates of 2·6 to 11·0 m Myr^{-1} from valley floor bedrock straths, indicating that the Darling Scarp is a slowly eroding 'steady state' landform, without any significant contemporary relief production over the last several 100 kyr and possibly several million years. Knickpoint retreat rates determined from ^{10}Be concentrations at the bases of two knickpoints on small streams incised into the scarp are 36 and 46 m Myr^{-1}. If these erosion rates were sustained over longer timescales, then associated knickpoints may have initiated in the mid-Tertiary to early Neogene, consistent with early-mid Tertiary marginal uplift. Ongoing maintenance of stream disequilibrium longitudinal profiles is consistent with slow, regional base level lowering associated with recently proposed continental-scale tilting, as opposed to differential uplift along discrete faults. Cosmogenic ^{10}Be analysis provides a useful tool for interpreting the palaeoseismic history of intraplate near-fault landforms over 10^5 to 10^6 years. Copyright © 2010 John Wiley & Sons, Ltd.

KEYWORDS: cosmogenic nuclide; erosion rates; Australia; scarp

Introduction

Landscape evolution reflects the complex interplay between tectonics, lithology and climate (e.g. Burbank and Anderson, 2001). As geomorphically similar landscapes may arise from disparate processes, the origin and evolution of many landscapes has remained unresolved. This is particularly true for intraplate settings such as Australia, where low levels of tectonic activity make discerning tectonically active landforms from relict landforms particularly problematic. The Darling Scarp in Western Australia (Figure 1) is a prime example of such a region. The ~900 km long Darling Scarp is one of the most prominent geomorphic features on the Australian continent. The scarp is underlain by the Darling Fault, which has a prolonged geological history, involving dip-slip displacement of up to 12 km during the rifting of Greater India from the Western Australian Margin that took place during the breakup of Gondwana some 132 million year ago (Harris, 1994; Veevers, 2000). The Darling Scarp lies astride one of the most seismically active zones in Australia, termed the South-West Seismic Zone (SWSZ: Doyle, 1971; Leonard, 2008) (Figures 1a and 2a), which includes some of Australia's largest earthquakes (up to M_w 6·8) (Clark *et al.*, 2005; Sandiford and Egholm, 2008). Despite this, there is no historical record of seismicity nor documented evidence for Neogene fault movement along the scarp. The origin of the scarp therefore remains unclear. The question of whether the scarp is presently tectonically active, intermittently active, or inactive is of more than academic concern – since it is central to the assessment of earthquake hazard for Perth, one of Australia's major cities.

In recent times, the ability to quantify rates of landform evolution through new chronometers such as cosmic-ray produced ('cosmogenic') isotopes has added new ways to quantitatively understand landscape processes. Rates of

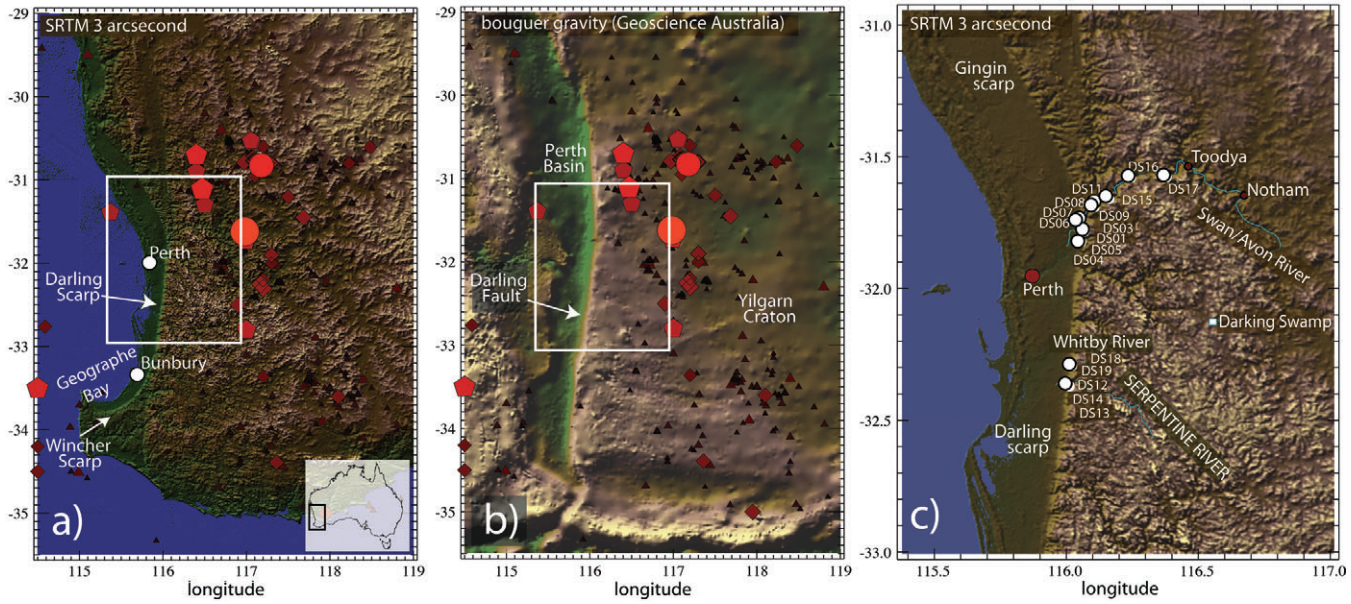

Figure 1. The Darling Scarp location and seismicity distribution maps; Legend: (M-earthquake magnitude) Circles: M = 6–7, Pentagons: M = 5–6, Diamonds: M = 4–5, Triangles: M = 2.5–4

a.) Detailed seismicity in SWSZ , Western Australia, showing all recorded events since 1910 overlayed on SRTM-3 arcsecond topography map (data obtained from Geoscience Australia database). The band of seismicity occurs inboard of the continental slope by ~200 km and shows no coincidence with the Darling Scarp and Whicher and Gingin Scarps that fork off from the Darling Scarp. Inset: map of Australia showing location of Darling Scarp. White circles represent town locations.

b.) The Bouguer gravity map of the Darling Scarp. The Bouguer gravity beneath the Perth Basin is ~100 mGal lower than the western Yilgarn Craton high.

c.) Detailed SRTM 3 arcsecond map of the field area (enclosed in the white frame in a & b) indicating locations of the cosmogenic sampling sites (white circles) in the Swan/Avon River and Whitby and Serpentine Rivers regions. The location of the Gingin Scarp is indicated. This figure is available in colour online at wileyonlinelibrary.com/journal/espl

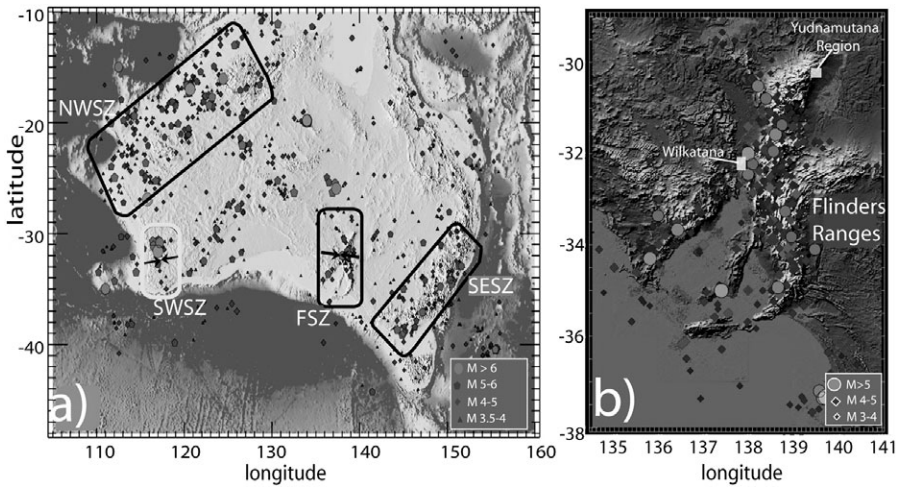

Figure 2. a.) Australian intraplate map overlayed on a topography map indicating four different seismic zones; North-West (NWSZ), South-west (SWSZ), Flinders (FSZ), and South-East (SESZ) seismic zone. The Darling Scarp is within the SWSZ, enclosed in the white frame in this figure. Note that the East-West compressional orientation direction in the modern stress field is present in both, the FSZ and SWSZ (Sandiford and Quigley, 2009; Hillis and Müller, 2003).

b.) Detailed historical seismicity pattern in the FSZ, South Australia, overlayed on SRTM-3 arcesond topography map, showing strong correspondence between earthquake distribution and the ranges. (M-earthquake magnitude).

escarpment evolution have been deduced from the measurement of cosmogenic nuclides in bedrock material outcropping along the escarpment (Heimsath *et al*., 2006; Fleming *et al*., 1999; Bierman and Caffee, 2001). For example, in the African landscape, cosmogenic analysis of the Drakensberg escarpment on the southeast African passive margin, indicate that the rates of summit denudation (6 m Myr^{-1}) are an order of magnitude lower than escarpment retreat rates (50–95 m Myr^{-1}) (Fleming *et al*., 1999) and that these low rates of summit denudation are sufficient to prevent the preservation intact of erosion surfaces over geological time (Fleming *et al*., 1999). Similar studies of cosmogenic analysis on the Namibian landscape (Bierman and Caffee, 2001) indicate that the landscape is experiencing steady and slow erosion rates, and that the Namibian escarpment has been undergoing this erosional behaviour since the continental break-up from South America, some 130 Myr ago. Heimsath *et al*. (2006) used cosmogenic isotope data from across the passive margin escarpment of south-eastern Australia to quantify erosion rates and processes from low-relief coastal lowlands to the highlands above the escarpment. Heimsath *et al*. (2006) found erosion rates near the escarpment base to be ~ 35 m Myr^{-1} and 3 m Myr^{-1} at the escarpment crest, demonstrating that erosion rates decrease with elevation from escarpment base to the summit. From beryllium-10 (^{10}Be) and Aluminium-26 (^{26}Al) cosmogenic analysis, Heimsath's *et al*. (2006) further suggest that the passive margin escarpment of south-eastern Australia has been relatively stable after having retreated rapidly immediately following the rifting between Australia and New Zealand 85–100 Myr ago. In addition,

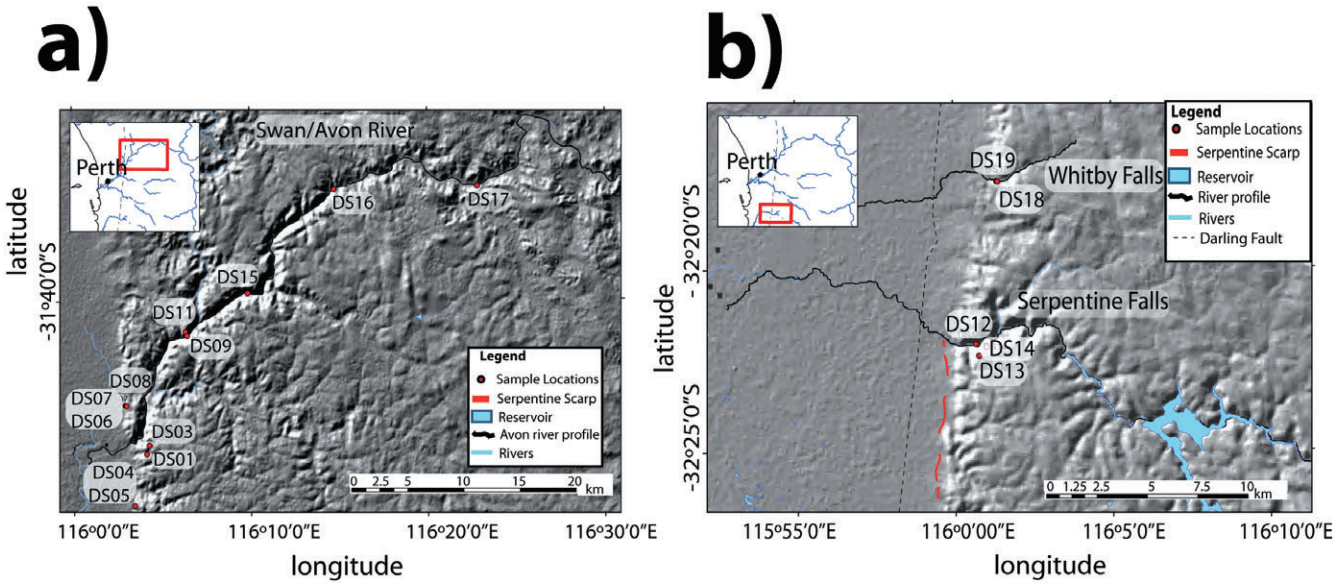

Figure 3. Digital elevation map (DEM) of the sample sites; Each sample location is indicated by sample names (eg. DS17- sample 17, labelled by red circles); Black dotted line- Darling Fault; Red curved dotted line -Serpentine Scarp; Blue represent Rivers/ Streams and River reservoir; Black line represents the River Profile (see Figure 5 for details on river Profile):
a.) Detailed DEM image of Avon/Swan River sample site showing the river profile, its incision into the Darling Ranges and sample locations within the site.
b.) Detailed DEM image of Whitby and Serpentine Falls sample sites indicating 900m Serpentine Falls incision into the Darling Ranges. Inset: map of Darling Ranges and Perth surroundings showing location of sample sites. This figure is available in colour online at wileyonlinelibrary.com/journal/espl

ongoing relief production along seismically active scarps has been demonstrated by differences in erosion rates between ridge tops and valley floors in uplifted fault blocks in the Flinders Ranges in South Australia. There, Quigley *et al*. (2007a, 2007b) used cosmogenic nuclide concentrations in bare bedrock surfaces to determine erosion rates on time scales of 10^3 to $>10^6$ years (see also Bierman and Caffee, 2002; Small *et al*., 1997). Quigley *et al*. (2007a) found erosion rates of up to 100 m Myr^{-1} in valley bottoms that were significantly higher than erosion rates from adjacent hill tops (average ~10 m Myr^{-1}). Relief production rates determined by cosmogenic analysis were shown to be consistent with independent constraints on fault slip rates at longer timescales. Such high rates of valley incision can be attributed to ongoing tectonic relief generation, reflecting the impact of seismic activity on slope stability. Many studies have shown a relationship between erosion rates, relief, incision, rock type and topography (Wobus *et al*., 2006; Ouimet *et al*., 2009; Schmidt and Montgomery, 1995; Burbank *et al*., 1996; Montgomery and Brandon, 2002; Safran *et al*., 2005). For example, Schmidt and Montgomery (1995) demonstrated that the relief of mountain ranges can reflect the interaction of valley incision and rock uplift and that the mountain-scale rock strength may also limit relief development in bedrock landscapes. Roering (2008) postulates through the model on hillslope evolution and topography that steady-state hilltop convexity varies non-linearly with the ratios of erosion rate to maximum soil production rate. Ouimet *et al*. (2009), using ^{10}Be cosmogenic data from the eastern margin of the Tibetean Plateau, suggest that variations in channel steepness 'drive landscape adjustment to increasing rates of base-level fall in tectonically active settings' (Ouimet *et al*., 2009, p. 582).

Building on the notion that active tectonic processes within intraplate settings can be discerned by measuring spatial variability in bedrock erosion rates (e.g. Quigley *et al*., 2007a, 2007b), this study uses analysis of ^{10}Be cosmogenic nuclide concentrations in bedrock exposures to quantify rates of relief production associated with the Darling Scarp (Figures 3a and 3b). We describe and compare the erosional processes operating at summit surfaces, hillslopes (scarp face), knickpoints and bedrock straths at the base of an active stream channel (Figures 4a–4d). Digital elevation model (DEM) data at 10 m and 20 m resolution are used to construct stream longitudinal profiles for the three streams from which samples were obtained. The results are used to evaluate the rates and mechanisms of scarp retreat, and the significance of convex longitudinal profiles that characterize the west flowing streams crossing the Darling Scarp.

Study Area

The Darling Scarp is a north-south linear structure that extends from Cape Naturaliste northwards some 900 km to the area east of Shark Bay. Maximum scarp relief is ~300 m in the southern segment inland from Bunbury and Perth, and diminishes gradually northwards. Geologically, the scarp extends alongside, and at some places overlaps, the Darling Fault, separating the Archean Yilgarn Craton to the east from the younger Pinjarra Orogen and overlying Phanerozoic Perth Basin to the west (Beard, 1999). The Perth basin sediments are up to 15 km thick siliclastic sediments produced by rifting between Australia and Greater India in the Early Permian-Early Cretaceous (Harris, 1994; Clark, 2008). Overlying the Perth Basin sediments are 30–70 m thick Quaternary and late Tertiary sands, clay and dune limestone (Clark, 2008). The Yilgarn Craton comprises deeply weathered and deformed Archean sedimentary and felsic-mafic-ultramafic volcanic and intrusive rocks set within larger areas of weakly metamorphosed and deformed granites (de Broekert and Sandiford, 2005). The Darling Fault is one of the major crustal structures in the Australian continent, with an associated ~100 mgal Bouguer gravity anomaly (Figure 1b) reflecting thick accumulations (up to 15 km) of low density Palaeozoic and Mesozoic sediment in the Perth Basin (Harris, 1994; Veevers, 2000). The Darling Scarp forms the main strand of a scarp complex that includes

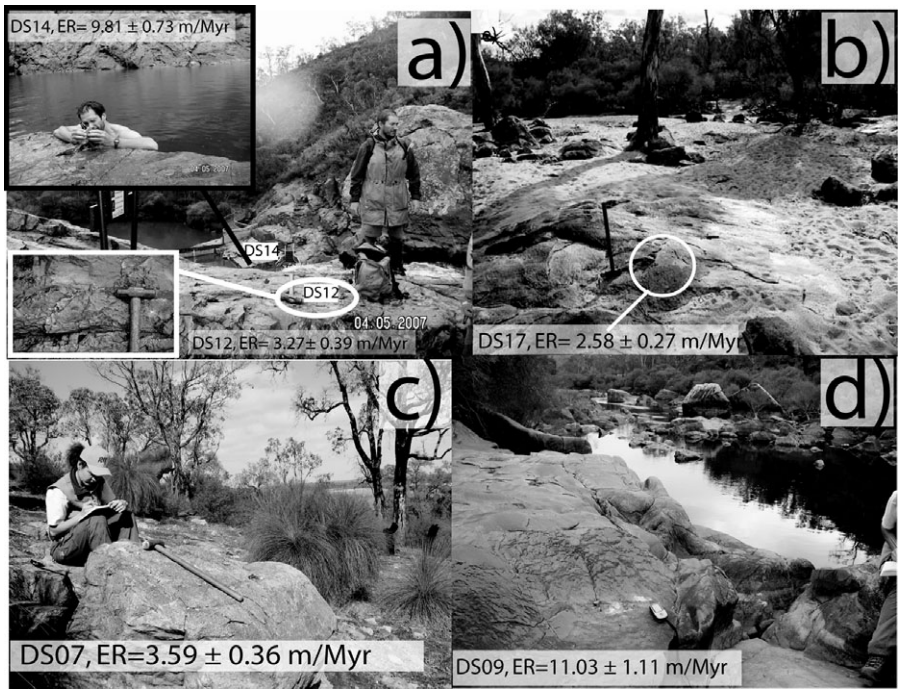

Figure 4. Selected cosmogenic sampling sites (denoted by arrows);
a.) Samples DS12-DS14 collected at the lip and base of the Serpentine River knickpoint (view towards the west). Insets: Shielding measurements taken at DS14 sample location, detailed view of the surface where the sample was taken from (view into the Serpentine knickpoint).
b.) Sample DS17 river strath bedrock sample collected at the position of the current stream level surrounded by stream sediments indicating possible multiple reburial events (view into the ranges, upstream the Awon/Swan River to the east).
c.) Sample DS07, scarp face sample collected from the north-west side of Swan/Avon River (view to the east into the scarp face).
d.) Sample DS09, river strath bedrock sample collected from the bedrock along Swan/Avon River at the same elevation as the maximum water rise, typically about 1·5 m above the current stream level. Down the stream view, direction to the west.

several smaller scarp splays. About 160 km south of Perth and inland of Bunbury, the Whicher Scarp branches southwest from the Darling Scarp and curves gently to reach the coast in Geographe Bay (see Figure 1a). Some 40 km north of Perth, the Gingin Scarp forks to the northwest where it cuts into Jurassic and Cretaceous sediments of the Perth Basin (Beard, 2003) (Figure 1c).

Located directly to the east of Perth, the Darling Scarp defines the western flank of the Darling Ranges. The origin of the Darling Ranges has been debated since King (1962) first postulated the existence of a 'marginal swell' based on differential elevations between inselbergs in the ranges and those at somewhat lower elevations further east. Beard (2003) argued that the Darling Ranges formed due to uplift of 150 to 200 m in a belt of 60 to 80 km immediately east of the scarp that resulted in major diversions of westerly flowing rivers crossing the range. Rivers have been cut and diverted into new channels or into already existing rivers [see Beard (2003) for more details on river diversion and their directions]. The notion of drainage derangement was first proposed by Mulcahy *et al*. (1972) who argued that the Avon-Swan River system previously flowed across what is now the Darling Range through a valley presently occupied by the Darkin Swamp (Figure 1) and has been diverted further north into a new channel through the Darling Ranges. Late Eocene fluviatile sediments preserved in disrupted palaeo-drainages along the eastern side of the Darling Ranges suggest mid-Tertiary uplift (Beard, 1999, 2003). This interpretation is further supported by an analysis of inset-valleys on the Yilgarn Craton. De Broekert and Sandiford (2005) showed that incision of these remarkable inset valley systems occurred in the early Middle Eocene in response to lowered geomorphic base-level and increased stream gradients affected by epeirogenic uplift of the Yilgarn Plateau. Wyrwoll (2003) argued that there has been no significant displacement across the Darling Fault during the Quaternary and perhaps also the late Tertiary. Beard (2003) interpreted the subsidiary Whicher and Gingin scarps as marine-cut landforms formed during Quaternary high sea stands.

Structural, stratigraphic, and geomorphic evidence in the earlier studies suggests that the Darling Scarp formed in the mid-Tertiary, when it was a tectonically active, uplifting landform with actively diverting river channels. The studies further agree that there has been no significant tectonic activity across the Darling Scarp since the Quaternary. However, the disequilibrium longitudinal profile observed in contemporary rivers, the proximity of the scarp to one of the most active seismic zones in Australia, and the favourable orientation of the underlying fault to be active with the contemporary stress field, all suggest that a more youthful tectonic influence on the scarp geomorphology is possible.

We obtained longitudinal profiles from six streams that cross the Darling Scarp, including the three streams sampled for cosmogenic analysis (Figures 5a–5d). These profiles show markedly convex profiles in proximity to the scarp face. The extent of the over-steepened reaches upstream of the scarp face increases with increasing catchment size. For example, the Swan/Avon River profile is convex within ~80 km of the scarp face (Figure 5c) and its catchment size is 105 000 km^2, whereas the Serpentine River is only over-steepened within 40 km of the scarp face and its catchment area is only 775 km^2 (Figure 5b).

The region immediately east of the Darling Scarp is one of the most active zones of seismicity in Australia (Figures 1 and 2a). Seismicity in the so-called SWSZ occurs within 30 km of the Darling Scarp (Figure 2a). This zone includes two of the largest earthquakes recorded in Australia (Gordon and Lewis, 1980). This seismicity records east-west compression associated with the Australian intraplate stress field (Hillis *et al*., 2008). The possible causes of enhanced seismicity in the

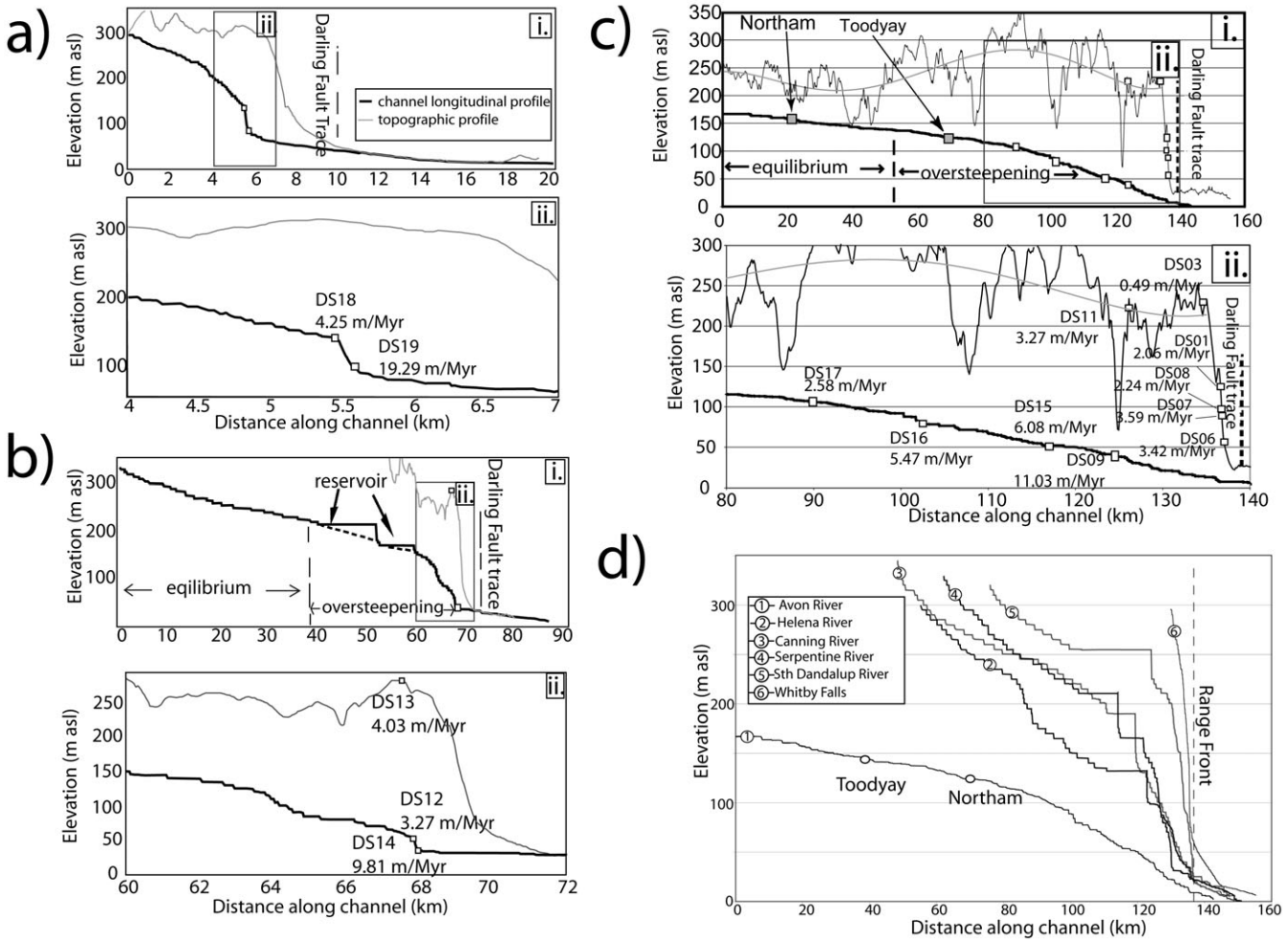

Figure 5. Darling Scarp longitudinal stream profile demonstrating slope replacement behaviour of the knickpoint migration. The profiles are constructed using 10 m and 20 m DEM data obtained from the Western Australian Department of Land Information, Landgate.
Legend: Black (tick) line- channel longitudinal profile; Grey line- topographic profile; Black dotted line- Darling Fault Trace; White squares- sample location
a.) i. Whitby River longitudinal and topographic profiles showing steep slope of the knickpoint migration.
ii. Detailed profile of the lip of the Whitby River knickpoint with mapped sample locations along the slope.
b.) i. Serpentine River longitudinal and topography profiles demonstrating how knickpoint migration decreases the channel gradient as it propagates further into the Darling ranges.
ii. Detailed profile of the lip of the Serpentine River knickpoint with mapped sample location along the slope, and the location of the sample from the summit surface above and to the south of the Serpentine River knickpoint.
c.) i. Avon/Swan river system topography and longitudinal profiles;
ii. Detailed profile of the lip of knickpoint of Avon/Swan river system. Nearly uniform slope without a clear knickpoint demonstrates a slope replacement erosion of the scarp migration. Convex profile (oversteepening) of the Avon/Swan is well represented in this image.
d.) A plotted diagram of all Darling Scarp stream profiles, equating the catchment size and stream power for the time evolution of the knickpoint retreat through the Darling Ranges (see text for details). In this image it is well demonstrated how the Darling Scarp erosion evolves through slope replacement.

SWSZ has been addressed recently by Sandiford and Egholm (2008) who suggested that the seismicity may reflect lithospheric weakening attendant with the thermal structuring of the continental margin. Sandiford and Egholm (2008) used thermo-mechanical models to show how lateral heat flow induced by variations in lithospheric thickness across the continent-ocean transition contributes to a maximum in Moho temperature and a minimum in lithospheric strength up to ~100 km inboard of the transition. Although the Darling Scarp has a long history of Palaeozoic to Mesozoic dip-slip movement and is oriented north-south, and thus in a favourable orientation to be active within the modern stress regime (Harris, 1994; Sandiford and Egholm, 2008; Hillis *et al*., 2008), there is no historical record of seismicity along it, nor any published indication of Neogene movement (e.g. Wyrwoll, 2003). Sandiford and Egholm (2008) postulated that because the Darling Scarp coincides with the strongest gradients in lithospheric and crustal thickness along the margin, and because it lies between the continent-ocean transition and the region of maximum Moho temperature, seismicity has been partitioned further inboard in the weaker region of the SWSZ (Sandiford and Egholm, 2008).

Rates of Bedrock Erosion from Cosmogenic ^{10}Be Dating

Methods

The Darling Ranges comprises a relatively homogeneous basement geology dominated by exposures of granite. The granite is fine to coarse grained, grouped into several batholiths, and

Table I. Cosmogenic erosion rates and exposure ages from ^{10}Be concentrations in bedrock samples along the Darling Scarp, Western Australia

Sample	Location (°S/°E)	Elevation (m asl)	Thickness (cm)	Production rate (atoms g^{-1} yr^{-1})		Shielding factor	[^{10}Be] ±σ[^{10}Be] (10^3 atoms g^{-1})	Erosion rate ±σ[^{10}Be] (m Myr^{-1})	Exposure age ±σ (ka)
				Spallation	Muons				
Summits									
DS03	31·778/116·071	206	1	4·9	0·211	0·999	4219 ± 155	0·49 ± 0·07	1051 ± 127
DS11	31·691/116·106	235	1	5·01	0·213	0·999	1067 ± 84	3·27 ± 0·41	216 ± 27
DS13	32·373/116·013	226	1·5	5·01	0·212	0·997	893 ± 53	4·03 ± 0·43	181 ± 20
Scarp face									
DS01	31·785/116·069	144	1	4·65	0·206	0·999	1454 ± 79	2·06 ± 0·24	324 ± 36
DS04	31·825/116·057	95	1	4·41	0·203	00·986	912 ± 101	3·48 ± 055	208 ± 31
DS05	31·825/116·057	95	1·5	4·41	0·203	0·986	891 ± 40	3·57 ± 0·35	204 ± 21
DS06	31·748/116·049	56	1	4·28	0·200	0·991	902 ± 70	3·42 ± 0·43	212 ± 26
DS07	31·748/116·049	85	1·5	4·36	0·202	0·983	878 ± 73	3·59 ± 0·47	204 ± 16
DS08	31·748/116·050	95	1	4·45	0·203	0·996	1309 ± 161	2·24 ± 0·40	303 ± 49
Bedrock straths (Swan/Avon River)									
DS09	31·694/116·107	38	2·5	3·93	0·199	0·923	313 ± 28	11·03 ± 1·35	78 ± 10
DS15	31·661/116·164	51	1	4·22	0·200	0·980	552 ± 83	6·08 ± 1·17	129 ± 23
DS16	31·581/116·246	79	2·5	4·28	0·202	0·972	606 ± 39	5·47 ± 0·59	142 ± 16
DS17	31·579/116·381	116	1·5	4·49	0·204	0·988	1177 ± 58	2·58 ± 0·27	270 ± 29
Knickpoints (Serpentine and Whitby Rivers)									
DS12	32·368/116·012	61	2	3·98	0·200	0·911	880 ± 86	3·27 ± 0·48	224 ± 31
DS14	32·368/116·011	23	1·5	3·48	0·198	0·822	321 ± 21	9·81 ± 1·00	90 ± 10
DS18	32·294/116·023	127	2·5	4·47	0·205	0·968	775 ± 94	4·25 ± 0·71	176 ± 27
DS19	32·294/116·023	105	1	4·04	0·204	0·890	197 ± 18	19·29 ± 2·30	47 ± 6

Note: Uncertainties are reported at the 1σ confidence level. Erosion rates, exposure ages and their uncertainties were calculated with the Cosmic-Ray Produced Nuclide Systematics (CRONUS) (http://hess·ess·washington·edu) Earth online calculator (Balco *et al*., 2008) version 2·1.

is heterogeneous with respect to deformation and lithology (Wilde and Nelson, 2001). For more detailed petrological description of the Darling Scarp granites please refer to Baxter and Doepel (1973). The granite is nearly continuously exposed at all elevations through the study area; as bedrock straths along the meandering course of the Swan/Avon River, Serpentine and Whitby falls; as scarp faces and hillslopes of all aspects; and as large bedrock tors on hillslopes, scarp face and summit areas. The Darling Ranges thus provide an excellent opportunity to quantify bedrock erosional processes from a variety of different geomorphic settings within a relatively lithologically homogenous system (Figures 4a–4d). To this end we have analysed 19 quartz samples collected from the uppermost few centimetres of bedrock surfaces. Samples taken on the summit surfaces, scarp face (samples DS01 to DS08) come from outcrops that have experienced millimetre to centimetre scale exfoliation (as interpreted from thicknesses of exfoliating weathering 'sheets'), grain by grain feldspar dissolution, and exhibiting strongly developed rock varnish, indicating very slow erosion rates.

Samples from fluvially-polished surfaces in channels (DS09, DS10, DS15 and DS16) were collected from the base of the active stream channel at maximum elevations of ~1·5 m above the current stream level. Sample DS09 was obtained from highly polished and incised bedrock at ~1·5 m above stream level, whereas sample DS17 was taken from bedrock only 2–3 centimetres above adjacent fine-grained stream sediments, in order to compare results from slightly different stream positions (Figure 4d).

At Serpentine Falls, samples have been collected at both the base and the lip of the knickpoint, as well as on the summit surface above the falls (Figure 4a). Sample DS12 was taken from a fluvially-polished exposure at the knickpoint ~20 m above the main stream. Sample DS13 was taken from the summit to the south of the falls. Sample DS14 was from a fluvially-polished bedrock strath at the base of the falls, about 1–2 m above the mainstream level (Figure 4a). At the Whitby Falls knickpoint, samples have been collected at the base (DS19) and at the lip (DS18) of the falls.

All scarp face and summit surface samples were collected from horizontal to subhorizontal bedrock surfaces displaying evidence of millimetre- to centimetre-scale exfoliation (Figures 4a–4d). Surface orientation, topographic shielding measurements, sample thicknesses and elevations for each sample are listed in Table I. Samples were crushed and the 250–500 μm fraction selected for analysis. Heavy-liquid separation was employed to isolate the quartz fraction, and the quartz was purified and beryllium extracted using the methods of Kohl and Nishiizumi (1992). For the beryllium cosmogenic nuclide analysis, the thickness of the sample is important when obtaining the data since cosmogenic ^{10}Be forms in near-surface materials by nuclear interaction between neutrons and muons. The production rate by nucleons decreases exponentially with depth below the surface, with mid-latitude penetration length of ~165 g cm^{-2} (Gosse and Phillips, 2001). Hence, at depths greater than ~60 cm the surface production rate has decreased by factor of *e* (Gosse and Phillips, 2001). Production rates due to muons attenuates more slowly than that due to neutrons, and becomes more relevant to total ^{10}Be production at depths greater than ~60 cm (Masarik and Reedy, 1995; Fabel, 2006). The effective attenuation length for production by high-energy spallation in rock of 160 g cm^{-2} is used (Gosse and Phillips, 2001; Balco *et al*., 2008) for Darling Scarp cosmogenic measurements. Typically, 0·3 mg of ^{9}Be carrier was added to each sample before quartz dissolution. The ^{10}Be/^{9}Be isotopic ratios were measured using accelerator mass spectrometry (AMS) on the 14UD accelerator at the Australian National University (ANU). Erosion rates were determined using the online Cosmic-Ray Produced Nuclide Systematics (CRONUS) calculator version 2·1 (http://hess.ess.washington.edu/math/) (Balco, 2007; Balco *et al*., 2008; Lal, 1991; Stone, 2000). A reference ^{10}Be cosmogenic nuclide production rate for the St scaling scheme of 4·96 ± 0·43 atoms g^{-1} year^{-1} (Balco *et al*., 2008) was used. Beryllium measurements were

Table II. Cosmogenic erosion rates and exposure ages from ^{10}Be concentrations in bedrock and alluvial samples, Flinders Ranges, South Australia (adopted from Quigley *et al*., 2007a)

Sample	Elevation (m)	Latitude (dec deg)	[^{10}Be] (10^3 atoms g^{-1})	σ[^{10}Be] (10^3 atoms g^{-1})	Erosion rate (m Myr^{-1})	σ (Erosion rate) (m Myr^{-1})	Exposure age (zero erosion) (ka)	σ (Exposure age (ka)
Summit surface								
YG06	389	30·19	236	18	19·61	2·08	42·87	4·05
SIL01	666	30·2	304	21	17·85	1·81	44·15	3·97
Bedrock benches								
YG03	285	30·19	177	19	25·04	3·31	35·07	4·3
YG04	334	30·19	112	15	42·14	6·53	21·19	3·13
YG05	374	30·19	151	20	31·65	4·91	27·63	3·97
SIL02	626	30·2	188	16	28·9	3·22	28·51	2·96
Knickpoints and strath								
YG02	254	30·19	184	19	22·65	2·88	39·23	4·51
YG08	231	30·19	90	11	44·51	6·36	22·56	3·08
YG01	242	30·19	30	16	157·44	51·99	6·34	3·449
Alluvial sediment								
YG07	229	30·19	137	14	33·02	4·15	27·15	3·25
Southern cliff face								
SF01	305	30·19	74	10	41·37	6·33	32·74	4·79
SF02	358	30·19	52	11	60·43	14·37	19·18	4·15
SF03	345	30·19	125	15	0	0	50·62	6·75
Eastern cliff face								
EF01	324	30·19	321	24	7·33	0·83	144·37	13·24
EF02	320	30·19	111	14	28·38	4·25	44·02	6·02

Note: Results differ slightly from Quigley *et al*. (2007a) since they have been recalculated using the online CRONUS calculator, version 2·1.

standardized to NIST_30000 (National Institute of Standards and Technology, NIST, with the isotope ratio of $3{\cdot}0 \times 10^{11}$) standards (Balco, 2007; Balco *et al*., 2008).

Results

The results for ^{10}Be concentrations and the corresponding bedrock erosion are presented in Table I. Bedrock erosion rates vary from ~0·5 to 4·0 m Myr^{-1} for summit surfaces, ~2·1 to 3·6 m Myr^{-1} for scarp faces and ~2·6 to 19·29 m Myr^{-1} for river channels (Table I). Because the summit and scarp face surface samples were collected from emerged, weathered top surfaces, the ^{10}Be concentrations are interpreted to provide maximum constraints on the rates of surface denudation. The consistent and low erosion rates found at all sample sites indicate very slow and spatially uniform erosional behaviour across the Darling Scarp. Importantly, these results imply river channel incision rates are not significantly higher than hillslopes (scarp face) erosion rates, and only marginally greater than summit surface lowering. The observation that erosion rates are similar across different landscape elements sampled implies that the shape of the scarp is being essentially preserved as it retreats.

The lowest erosion rates at the Serpentine and Whitby Rivers are 3·3 and 4·3 m Myr^{-1}, respectively, and are consistent with the erosion rates observed from samples in the Swan/Avon River (Table I). The highest erosion rate measured is 9·8 and 19·29 m Myr^{-1} respectively, located at the base of the Serpentine and Whitby Rivers knickpoints.

Discussion

Implications of cosmogenic data for escarpment evolution and origin

The ^{10}Be analyses from the Darling Scarp presented here reveal that uniformly low erosion rates characterize different landscape components and suggest that there has been no significant relief generation across the scarp over the timescale probed by the cosmogenic nuclide ^{10}Be inventories (in this case, $\geq 10^5$ to 10^6 years). In concert with the dearth of evidence for any Quaternary tectonic activity, these results are interpreted as evidence that the Darling Scarp is a slowly eroding landform that has not experienced any major earthquake events (that would have episodically removed bedrock and lowered ^{10}Be concentrations) over the last several 10^5 years, and possibly longer. The prominent geomorphic expression of the Darling Scarp thus relates to the slow modification of a previously formed topographic anomaly, rather than a landform created by contemporary faulting.

The relationship between seismic activity and erosion rates in intraplate settings such as Australia is not well understood, reflecting the paucity of robust quantitative measures for both erosion rate and seismic activity. While the low level of seismic activity in intraplate settings means that quantitative measures of seismic moment release are subject to large uncertainties, several studies have now attempted to quantify moment release rates (e.g. Sandiford *et al*., 2004; Celerier *et al*., 2005; Braun *et al*., 2009; Leonard, 2008). These studies show seismic strain rates vary within the continent by over one-order of magnitude (from $<10^{-17}$ s^{-1} to ~10^{-16} s^{-1}), and that in areas such as the Flinders Ranges, relatively high seismic strain rates are compatible with longer term fault slip rates deduced from neotectonic studies (Sandiford, 2003a, 2003b). The Flinders Ranges therefore provide an important counterpoint to the Darling Scarp (Quigley *et al*., 2006; Sandiford and Egholm, 2008) (Figures 2a and 2b). Both regions exhibit granite bedrock of relatively steep hillslopes, in semi-arid environments, with distinctly different levels of seismic activity. Recent cosmogenic studies in the Flinders Ranges have demonstrated significant differences in erosion rates from ridge tops and valley floors in the uplifted fault blocks (Table II). Quigley *et al*. (2007a) measured erosion rates of ~14 m Myr^{-1} on multiple summit surfaces and >100 m Myr^{-1} in valley bottoms in the Yudnamutana region of the Northern Flinders Ranges. In the Wilkatana area situated along the western flank

of the central Flinders Ranges, erosion rates vary from ~6 m Myr^{-1} on ridge crests to ~50 m Myr^{-1} in adjacent valley floors (Quigley *et al.*, 2007b). With present-day tectonic relief generation estimated at rates of at least 50 m Myr^{-1} (Sandiford, 2003a; Quigley *et al.*, 2007a), the Flinders Ranges data clearly contrasts with our new data from the Darling Scarp, revealing an old landscape with negligible active relief production (Tables I and II). Notably, our highest measured erosion rate of 19 m Myr^{-1} from the base of the knickpoint at Whitby Falls (DS19 = 19·29 m Myr^{-1} see Table I) is much lower than all measured valley bottom erosion rates from the Flinders Ranges. In as much as the Flinders Ranges and Darling Scarp occupy similar semi-arid climates (although the former is more arid), have the same bedrock type (although some studies in the former are within quartzite terranes), and have similar aspects and slopes, the obvious distinction lies in the level of seismic activity, suggesting that cosmogenically-derived erosion rates can be used to assess relative rates of neotectonic activity even within mildly deforming intraplate settings such as Australia.

Knickpoint propagation and the age of scarp relief

Interpretation of the ^{10}Be concentrations from the base of the Serpentine and Whitby Rivers knickpoints is complicated, given that these samples may have undergone complex exposure histories including partial burial by stream sediment given their positions at the base of waterfalls. Additionally, it is unclear how the 'erosion rate' obtained from these samples relates to a 'steady-state' erosion rate, as they may have been exposed during prior knickpoint propagation over the sample site, hence resulting in a lower ^{10}Be concentration compared to other, actively eroding parts of the stream bed. For this reason, we interpret these rates as maximum stream incision rates at a point, as opposed to regional stream-downcutting rates (Figure 6a). We then use these point measurements to determine maximum knickpoint lateral retreat rates. The evolution of knickpoints in the Swan/Avon and Serpentine and Whitby streams provides a useful framework for assessing the timescale of the evolution of the Darling Scarp that has taken place since these knickpoints were initiated. To estimate the timing of their initiation requires an understanding of how these knickpoints are likely to have developed through time.

As shown in Figure 6(b), three end-member models describe how knickpoints propagate (Gardner, 1983; Burbank and Anderson 2001):

(i) parallel retreat of the knickpoint through time with the initial shape being maintained;
(ii) knickpoint propagation in uniformly resistant rocks with slope replacement during migration;
(iii) knickpoint formation and propagation controlled by differential erosion of strata with contrasting resistance to erosion.

The fundamental difference between the models relates to whether the original shape of the knickpoint is amplified in a vertical sense, simply translates through the landscape, or whether it smooths and flattens during translation (Figure 6b). Wobus *et al.* (2006) postulate in their studies on fluvial systems that the stream profile analysis is an invaluable qualitative tool for neotectonic studies. They illustrate that in northern and southern California, channel steepness is directly related to rock uplift rates and show that changes in steepness and concavity in Siwalik Hills in Nepal correlate with rock uplift rate variation (Wobus *et al.*, 2006). Similarly, Crosby and Whipple (2006) have shown through their models of the knickpoint initiation and distribution within fluvial networks that the knickpoint retreat distances were

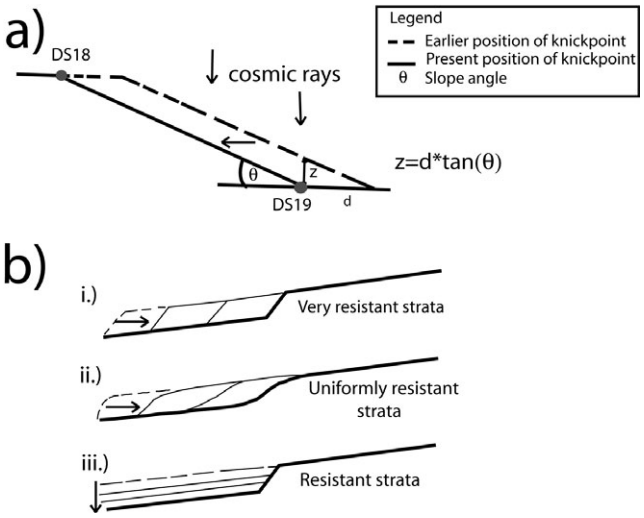

Figure 6. *a.)* Illustration of knickpoint retreat behaviour. With the knickpoint at the earlier position, production of ^{10}Be of the base sample (DS19 in this example) is occurring under z cm of rock. Hence, production rate $P_{(Z)} = P_{(0)} * e^{(-Z/\mu)}$, where μ is the attenuation length (~60 cm). As the knickpoint moves to the left, z decreases and the production rate therefore increases. The current slope angle, θ, of the knickpoint is used to calculate horizontal retreat of the knickpoint. Retreat Rate = distance/exposure age.
b.) Knickpoint migration models after Burbank and Anderson (2000). The profile of the Darling Scarp mimics the slope replacement behaviour; see text and Figure 5 for more details.
i.) Parallel retreat
ii.) Slope replacement
iii.) Differential erosion without propagation

well correlated with tributaries drainage areas. They propose that the knickpoint retreat rate is a power law function of drainage area (see also Bishop *et al.*, 2005; Wobus *et al.*, 2006).

Following these studies, we use catchment size/stream power as a proxy for time in order to construct an evolutionary model for knickpoint retreat trough the Darling Ranges. Knickpoint migration is seen to evolve from steep (Whitby Falls) to less steep (Swan/Avon) (see Figures 5a–5d). When added to the mapped geology, which is dominated by crystalline Archaean granites (Lord, 1980), the profiles of all three catchment areas mimic the 'slope replacement' knickpoint migration model (Figure 6b (part ii) and Figure 5). Figure 5(a) shows that the originally steep knickpoint evolved through slope replacement into a reach of nearly uniform slope without a clear knickpoint (Figures 5b–5d). The knickpoint features shown in Figures 5(a)–5(d) are consistent with the Gardner (1983) knickpoint retreat experimental model and agrees with his statement of knickpoint retreat in homogenous bedrock; 'knickpoint replacement is a significant process in the evolution of knickpoints in homogenous bedrock . . . knickpoints do not undergo parallel headward retreat in homogenous bedrock' (Gardner, 1983, p. 664). Weissel and Seidl (1998) in their study on gorge head-knickpoint scarp propagation imply that the pattern of knickpoint erosion rate in the downstream direction corresponds to the inland scarp retreat across passive continental margins. They describe gorge head-knickpoint scarp as the scarp where streams flow across it towards the coast, as is the case with the Darling Scarp (see also Weissel and Seidl, 1997). Similarly, Seidl *et al.* (1996, p. 309) state in their study of knickpoints and pattern of scarp retreat '. . . the propagation of scarps through the continental landmass can be viewed as the upstream migration of large-scale knickpoints in bedrock

river'. From the earlier studies, it is fair to assume that scarps such as the Darling Scarp retreat following the pattern of their knickpoints propagation. This is further supported by King's (1953) model of landscape evolution and scarp retreat in semi-arid regions that has similar pattern as Gardner's (1983) model of knickpoints propagation.

Following Figure 6(a) with given slope angles of 10° and 23° for the Serpentine and Whitby knickpoints, respectively, and their vertical erosion rates of 9·81 m Myr^{-1} and 19·29 m Myr^{-1}, respectively, we derive knickpoint retreat rates of 46 m Myr^{-1} for the Serpentine knickpoint and 36 m Myr^{-1} for the Whitby knickpoint, where 'horizontal retreat rate' = 'vertical erosion rate'/'tan(slope angle)'. Similar arguments can be used to determine the retreat rate of the scarp itself from the ^{10}Be measurements on the slope of the scarp face. Assuming an average scarp face slope angle of 12·5°, and an average vertical erosion rate of the slope (3·09 m Myr^{-1}) the lateral retreat rate of the Darling Scarp is ~14 m Myr^{-1}. Although these 'rates' should be viewed with caution, they provide our best attempt at quantifying escarpment geomorphic evolution using point samples. Regardless of how the ^{10}Be inventories are treated, the concentration are significantly higher, and thus erosion rates significantly lower than those from tectonically active but more arid environments such as the Flinders Ranges (Quigley *et al*., 2007a, 2007b).

An important question that can be addressed indirectly from our new analyses is the age of the Darling Scarp relief. If we assume that the cosmogenic rates of knickpoint and scarp retreat are representative of the long term, then these rates can be used to estimate the time of knickpoint initiation. Given that these knickpoints are propagating through a fully developed valley system, their initiation must have post-dated formation of the scarp relief. The cosmogenic data show that the Serpentine falls, now ~950 m upstream of the Darling scarp (Figures 3b and 5b), is retreating at 46 m Myr^{-1}, while the scarp face itself is retreating at 14 m Myr^{-1}. Assuming the scarp face and the Serpentine falls coincided at time T ago, when the scarp face was at a distance D in front of its present position, then the falls have retreated D + 950 m in the same time that the scarp face has retreated D. Under these assumptions knickpoint initiation (time T) is then ~ 30 Myr ago when the scarp face was ~430 m further west of its current position. Applying the same logic to the Whitby knickpoint, which is presently 450 m behind the scarp face and retreating at ~36 m Myr^{-1}, yields an initiation time of ~21 Myr ago when the scarp face was ~294 m in front of its current position. Correspondingly, given that the scarp has retreated 2000 m from the Daring fault trace (see Figure 5; Wyrwoll, 2003) at a rate of 14 m Myr^{-1} (assuming the retreat rates are still representative of the long term), then the estimated time of faulting and relief creation on the scarp is ~143 Myr. Similar ages of ~142 Myr and ~143 Myr are obtained using the Serpentine and Whitby knickpoint retreat rates, respectively. Within the limitations of the assumption of constant rates, the initiation of the Serpentine knickpoint is consistent with Beard's (2003) suggested mid-Tertiary marginal uplift and the results of both knickpoint initiations support the argument that there has been no significant displacement along the Darling Scarp during the Quaternary. A word of caution is, however, required since at ~30 Myr ago, this region of Australia was at a latitude of ~45°S and the climate was likely substantially wetter than present (Martin, 2006). Hence, the assumption that the present day retreat rates of the knickpoints and scarp face are representative of the long term may be somewhat simplistic. Since erosion rates were likely to have been higher under a higher rainfall regime, the mid-Tertiary to early Neogene initiation obtained here are likely to be maximum values.

Tectonic implications of stream profiles and erosion rates

Streams in dynamic equilibrium, flowing across a uniform lithology, are observed to develop an exponential 'concave up' longitudinal profile (e.g. Hack, 1957, 1973; Goldrick and Bishop, 2007), unlike the 'convex up' profiles of the Darling Scarp streams (Figure 5). 'Convex up' or disequilibiurm profiles may be the result of a change in lithology along the profile, surface tectonic deformation, or a change in base level downstream of the convexity (McKeown *et al*., 1988; Goldrick and Bishop, 1995; Radoane *et al*., 2003). Yatsu (1955) argued that in the graded rivers, the balance between tractive force and bed maintains the equilibrium longitudinal profile, while discontinuous collapse at the grainsize will develop the convexity within the profile. The mathematical model by Radoane *et al*. (2003) disproved the theory of rivers achieving equilibrium longitudinal profile with age by showing that in contrary to the southern rivers of Carpathian (2·5 Myr), the northern rivers (13–14 Myr) were not able to achieve the equilibrium due to the convexity caused by tectonic uplift. The erosion rates calculated for the bed of the Swan/Avon River systematically decrease from a maximum of 11·03 m Myr^{-1} close to the scarp face (~11·4 km upstream beyond the scarp face), to a background level of 2·58 m Myr^{-1} near Toodyay (~47·14 km upstream beyond the scarp face). This suggests that the river is responding to base level change at or east of the scarp face. The apparent absence of any late Quaternary tectonic activity along the scarp suggests an alternative causative mechanism must be invoked to explain the disequilibrium.

A marked latitudinal asymmetry in Neogene stratigraphic records from around the Australian coastline implicates a long-term trend of north-down, south-southwest-up dynamic tilting of the continent since at least the mid-Tertiary, which can also be related to variations in dynamic topography and the geoid (Sandiford, 2007; Sandiford *et al*., 2009; Sandiford and Quigley, 2009). Along the southern coastline of Western Australia, the rate of uplift due to the postulated continental tilting is estimated to be between ~15–20 m Myr $^{-1}$. This rate is easily sufficient to maintain, and even enhance with time, disequilibrium longitudinal profiles of streams crossing the Darling Scarp (see earlier text and Figure 5), given that our data indicates that the Swan/Avon River system is incising into the Darling Ranges between 2·58 to 11·03 m Myr^{-1}. While a role for tectonism is not excluded by this data, activity on the Darling Fault is not required to explain the ubiquitous disequilibrium in stream longitudinal profiles. Hence, we attribute the formation and maintenance of disequilibrium stream longitudinal profiles crossing the Darling Scarp to slow, regional base level lowering associated with continental-scale tilting. This conclusion is consistent with the ^{10}Be cosmogenic results on the Darling Scarp itself, which indicates an ancient, tectonically inactive and stable feature.

Conclusion

Low cosmogenic ^{10}Be erosion rates and erosion rate variability from bedrock outcrops comprising the Darling Scarp imply minimal relief production over the Quaternary, consistent with this feature being a slowly eroding, tectonically inactive feature. Knickpoint retreat rates are compatible with long-term rates derived from geological constraints and, if representative of longer term rates, are consistent with the interpretation that knickpoints formed during early Tertiary tectonic uplift and have been slowly propagating through the landscape since

then. High cosmogenic ^{10}Be concentrations in active stream channels indicate slow erosion that is inconsistent with tectonically modulated incision along the adjacent range-front, as has been proposed for other Australian landscapes (e.g. Flinders Ranges), and is more consistent with a fluvial response to slow, long wavelength, low amplitude southwest side up tilting of the Australian continent. Continental tilting may explain the disequilibrium longitudinal profiles in streams incised into the Darling Scarp. Comparison of the ^{10}Be cosmogenic nuclide concentrations of the aseismic Darling Scarp with seismically active Flinders Ranges suggest that ^{10}Be nuclide analysis is a very useful tool in determining whether a structure, or region, has been tectonically active over the timescales of cosmogenic nuclide accumulation, thus providing a potential palaeo-seismic tool with a range of up to 10^5 to 10^6 years.

Acknowledgements—We thank Peter Hoiles, Sofia Chapman and Kaye Hannam for proofreads that improved the quality of this manuscript. Clark publishes with the permission of the CEO of Geoscience Australia. This research was supported by ARC grant DP055613.

References

Balco G. 2007. *CRONUS-Earth ^{26}Al–^{10}Be Exposure Age Calculator MATLAB Function Reference, Version 2·1,* November. University of Washington: Seattle, WA.

Balco G, Stone JO, Lifton NA, Dunai TJ. 2008. A complete and easily accessible means of surface exposure ages or erosion rates from ^{10}Be and ^{26}Al measurements. *Quaternary Geomorphology* **3**: 174–195. DOI. 10.1016/j.quageo.2007.12.001

Baxter JL, Doepel JJG. 1973. Geology of the Darling Scarp Between LLatitudes 32° and 33° south, W.A. *Geological Survey of Western Australia* **1966**(6): 1–8.

Beard JS. 1999. Evolution of the river systems of the south-west drainage division, Western Australia. *Journal of the Royal Society of Western Australia* **82**: 29–38.

Beard JS. 2003. Palaeodrainage and the geomorphologic evolution of passive margins in Southwestern Australia. *Zeitschrift für Geomorphologie* **47**: 273–288.

Bishop P, Hoey TB, Jansen JD, Artza IL. 2005. Knickpoint recession rate and catchment area: the case of uplifted rivers in eastern Scotland. *Earth Surface Processes and Landforms* **30**: 767–778.

Bierman PR, Caffee M. 2001. Slow rates of rock surface erosion and sediment production across the Namib Desert and escarpment, Southern Africa. *American Journal of Science* **301**: 326–358.

Bierman PR, Caffee M. 2002. Cosmogenic exposure and erosion history of Australian landforms. *GSA Bulletin* **114**: 787–803.

Braun J, Burbidge DR, Gesto FN, Sandiford M, Gleadow AJW, Kohn BP, Cummins PR. 2009. Constraints on the current rate of deformation and surface uplift of the Australian continent from a new seismic database and low-T thermochronological data. *Australian Journal of Earth Sciences* **56**: 99–110.

Burbank DR, Leland J, Fielding E, Anderson RS, Brozovic N, Reid MR, Duncan C. 1996. Bedrock Incision, rock uplift and threshold hillslopes in the northwestern Himalayas. *Nature* **379**: 505–510.

Burbank DW, Anderson RS. 2001. *Tectonic Geomorphology*. Blackwell Science: Malden, MA.

Celerier J, Sandiford M, Hansen DL, Quigley M. 2005. Modes of active intraplate deformation, Flinders Ranges, Australia. *Tectonics* **24**(6): 1–17. DOI. 10.029/2004andC001679

Clark D. 2008. *Field Investigation of Linear Scarps South of Perth, Western Australia: Relationships to Faulting*. Geoscience Australia Record: Sydney; 2006/XX.

Clark D, Dentith M, Wyrwoll KH. 2005. *Palaeoseismic Investigation of the Meckering Fault Scarp, Western Australia: Implications for the Style of Interplate Deformation*, External Publication, Geoscience Australia, 'Geospatial information for the nation'. Department of Industry, Tourism and Resources: Canberra.

Crosby BT, Whipple KX. 2006. Knickpoint initiation and distribution within fluvial networks: 236 waterfalls in the Waipaoa River, North Island, New Zealand. *Geomorphology* **82**: 16–38.

de Broekert P, Sandiford M. 2005. Buried inset-valleys in the eastern Yilgarn Craton, Western Australia: geomorphology, age and allogenic control. *Journal of Geology* **113**: 471–493.

Doyle HA. 1971. Australian seismicity and plate boundaries. *Nature Physical Science* **234**: 174–175.

Fabel D. 2006. *A Brief Introduction to* in-situ *Produced Terrestrial Cosmogenic Nuclide Methods*, CRC LEME Open File Report, Report no. 189. Australian National University: Canberra; 7–18.

Fleming A, Summerfield MA, Stone JO, Fifield LK, Cresswell RG. 1999. Denudation rates for the southern Drakensberg escarpment, SE Africa, derived from *in-situ*-produced cosmogenic ^{36}Cl: initial results. *Journal of the Geological Society, London* **156**: 209–212.

Gardner TW. 1983. Experimental study of knickpoint and longitudinal profile evolution in cohesive homogeneous material. *Geological Society of America Bulletin* **94**: 664–672.

Goldrick G, Bishop P. 1995. Differentiating the roles of lithology and uplift in the steepening of bedrock river long profiles: an example from southeastern Australia. *The Journal of Geology* **103**: 227–231.

Goldrick G, Bishop P. 2007. Regional analysis of bedrock stream long profiles: evaluation of Hack's SL form, and formulation and assessment of an alternative (the DS form). *Earth Surface Processes and Landforms* **32**: 649–671. DOI. 10.1002/esp.1413.

Gordon FR, Lewis JD. 1980. The Meckering and Calingiri Earthquakes October 1968 and March 1970. *Geological Survey WA Bulletin* **126**: 229.

Gosse J, Phillips FM. 2001. Terrestrial *in situ* cosmogenic nuclides: theory and application. *Quaternary Science Reviews* **20**: 1475–1560.

Harris LB. 1994. Structural and tectonic synthesis for Perth Basin, Western Australia. *Journal of Petroleum Geology* **17**: 129–156.

Hack JT. 1957. *Studies of Longitudinal Stream Profiles in Virginia and Maryland*, US Geological Survey Professional Paper 294-B. US Geological Survey: Reston, VA; 45–97.

Hack JT. 1973. Stream-profile analysis and stream-gradient index. *Journal of Research of US Geological Survey* **1**: 421–429.

Heimsath AM, Chappell J, Finkel RC, Fifield K, Alimanovic A. 2006. Escarpment erosion and landscape evolution in southeastern Australia. *Geological Society of America* **398**: 173–190.

Hillis RR, Sandiford M, Reynolds SD, Quigley MC. 2008. Present-day stresses, seismicity and Neogene-to-recent tectonics of Australia's 'passive' margins: intraplate deformation controlled by plate boundary forces. In *The Nature and Origin of Compression in Passive Margins*, Jonhson H, Dore AG, Gratliff RW, Holdsworth R, Lundin E, Ritchie JD (eds), Special Publications 306. Geological Society: London; 71–89.

King LC. 1953. Canons of landscape evolution. *Geological Society of America Bulletin* **64**: 721–752. DOI. 10.1130/0016-7606

King LC. 1962. *The Morphology of the Earth: A Study and Synthesis of World Scenery*. Oliver and Boyd: Edinburgh.

Kohl CP, Nishiizumi K. 1992. Chemical isolation of quartz for measurement of *in-situ*-reduced cosmogenic nuclides. *Geochimica et Cosmochimica Acta* **56**: 3583–3587.

Lal D. 1991. Cosmic ray labelling of erosion surfaces: in situ nuclide production rates and erosion models. *Earth and Planetary Science Letters* **104**: 424–439.

Leonard M. 2008. One hundred years of earthquake recording in Australia. *Bulletin of Seismological Society of America* **98**: 1458–1470.

Lord JH. 1980. *Pinjarra Geological Map*, Sheet SI 50-2 and part of Sheet SI 50-1, Scale 1 : 250 000. Geological Survey of Western Australia: Canberra.

Martin HA. 2006. Cenozoic climate change and the development of the arid vegetation in Australia. *Journal of Arid Environments* **66**: 533–563.

Masarik J, Reedy RC. 1995. Terrestrial cosmogenic nuclide production systematic calculated from numerical simulations. *Earth and Planetary Science Letters* **104**: 424–439.

McKeown FA, Jones-Cecil M, Askew BL, McGrath MB. 1988. *Analysis of Stream-profile Data and Inferred Tectonic Activity, Eastern Ozark Mountains Region*, US Geological Survey Bulletin B 1807. US Geological Survey: Reston, VA; 1–39.

Montgomery DR, Brandon MT. 2002. Topographic controls on erosion rates in tectonically active mountain ranges. *Earth and Planetary Science Letters* **201**: 481–489.

Mulcahy MJ, Churchward HM, Dimmock GM. 1972. Landforms and soils on uplifted penaplain in the Darling range, Western Australia. *Australian Journal of Soil Research* **10**: 1–14.

Ouimet WB, Whipple KX, Granger DE. 2009. Beyond threshold hillslopes: channel adjustment to base-level fall in tectonically active mountain ranges. *Geology* **37**(7): 579–582. DOI. 10.1130/G30013A

Quigley M, Cupper M, Sandiford M. 2006. Quaternary faults of southern Australia: palaeoseismicity, slip rates and origin. *Australian Journal of Earth Sciences* **53**: 285–301.

Quigley M, Sandiford M, Fifield K, Alimamovic A. 2007a. Bedrock erosion and relief production in the northern Flinders Ranges, Australia. *Earth Surface Processes and Landforms* **32**: 929–944. DOI. 10.1002/esp.1459

Quigley M, Sandiford M, Fifield LK, Alimamovic A. 2007b. Landscape responses to intraplate tectonism: quantitative constrains from ^{10}Be nuclide abundances. *Earth and Planetary Science Letters* **261**: 120–133. DOI.10.1016/j.epsl.2007.06.020

Radoane M, Radoane N, Dumitriu D. 2003. Geomorphological evolution of longitudinal river profiles in the Carpathians. *Geomorphology* **50**: 293–306.

Roering JJ. 2008. How well can hillslope evolution models 'explain' topography? Simulating soil transport and production with high-resolution topographic data. *GSA Bulletin* **120**(9/10): 1248–1262. DOI. 10.1130/B26283.1

Safran EB, Bierman PR, Aalto R, Dunne T, Whipple KX, Caffee M. 2005. Erosion rates driven by channel network incision in the Bolivian Andes. *Earth Surface Processes and Landforms* **30**: 1007–1024. DOI. 10.1002/esp.1259

Sandiford M. 2003a. Neotectonics of southeastern Australia: linking the Quaternary faulting record with seismicity and in situ stress. In *Evolution and Dynamics of the Australian Plate*, Hillis RR, Muller D (eds). Geological Society of Australia, Special Publication 22. Geological Society of Australia: Sydney; 101–113.

Sandiford M. 2003b. Geomorphic constrains on the late Neogene tectonics of the Otway Ranges. *Australian Journal of Earth Sciences* **50**: 69–80.

Sandiford M. 2007. The tilting continent: a new constraint on the dynamic topographic field from Australia. *Earth and Planetary Sciences Letters* **261**: 152–163. DOI. 10.1016/j.epsl.2007.06.023

Sandiford M, Wallace M, Coblentz D. 2004. Origin of the *in situ* stress field in southeastern Australia. *Basin Research* **16**: 325–338.

Sandiford M, Egholm DL. 2008. Enhanced intraplate seismicity along continental margins: some causes and consequences. *Tectonophysics* **475**: 197–208. DOI. 10.1016/j.tecto.2008.06.004

Sandiford M, Quigley MC. 2009. TOPO-OZ: insights into the various modes of intraplate deformation in the Australian continent. *Tectonophysics* **474**: 405–416. DOI.10.1016/j.tecto.2009.01.028

Sandiford M, Quigley M, de Broekert P, Jakica S. 2009. Tectonic framework for the Cainozoic cratonic basins of Australia. *Australian Journal of Earth Sciences* **56**: S5–S18. DOI. 10.1080/08120090902870764

Schmidt KM, Montgomery DR. 1995. Limits to relief. *Science* **270**: 617–620.

Seidl MA, Weissel JK, Pratson LF. 1996. The kinematics and pattern of escarpment retreat across the rifted continental margin of SE Australia. *Basin Research* **12**: 301–316.

Small EE, Anderson RS, Repka JL, Finkel R. 1997. Erosion rates of alpine bedrock summit surfaces deduced from *in situ* ^{10}Be and ^{26}Al. *Earth and Planetary Science Letters* **150**: 413–425.

Stone JO. 2000. Air pressure and cosmogenic isotope production. *Journal of Geophysical Research* **105B**: 23753–23759.

Veevers JJ. 2000. *Billion-year Earth History of Australia and Neighbours in Gondwanaland*. GEMOC Press: Sydney; 388.

Weissel JK, Seidl MA. 1997. Influenceof rock strength properties on escarpment retreat across passive continental margins. *Geology* **25**: 631–634.

Weissel JK, Seidl MA. 1998. Inland propagation of erosional escarpments and river profile evolution across the southeast Australian Passive Continental Margin. *Geophysical Monograph* **107**: 189–206.

Wilde SA, Nelson DR. 2001. Geology of the western Yilgarn Craton and Leeuwin Complex, Western Australia – a field guide. *Geological Survey of Western Australia* **Record 2001/15**: 1–41.

Wobus C, Whipple KX, Kirby E, Snyder N, Johnson J, Spyropolou K, Crosby B. 2006. Tectonics from topography: procedures, promise, and pitfalls. In *Tectonics, Climate, and Landscape Evolution*, Willett SD, Hovius N, Brandon MT, Fisher DM. Geological Society of America Special Paper, Penros Conference Series 398. 55–74. Geological Society of America: Boulder, CO. DOI. 10.1130/2006.2398(04)

Wyrwoll KH. 2003. The geomorphology of the Perth region, Western Australia. *Australian Geomechanics* **38**(30): 17–32.

Yatsu E. 1955. On the longitudinal profile of the graded river. *Transactions – American Geophysical Union* **36**(4): 655–663.